

The Influence of Left Atrial Wall Thickness and Curvature on Wall Strain in Patient-Specific Atrium Models

Tiffany MG Baptiste¹, Angela Lee¹, Marina Strocchi¹, Charles Sillett¹, Daniel B Ennis², Ulrike Haberland³, Ronak Rajani^{1,4}, Aldo Rinaldi^{1,4}, Steven A Niederer¹

¹King's College London, London, UK

²Stanford University, California, USA

³Siemens Healthcare Limited, Camberley, UK

⁴Guy's and St. Thomas' NHS Foundation Trust, London, UK

Abstract

Fibrosis is thought to be a major contributor to atrial fibrillation. Strain is a potential signal for fibrosis. Local strain can be impacted by local anatomy. This study investigated correlation of local strain magnitude with local anatomy described by curvature and wall thickness.

We created 3D motion models of the left atrium from retrospective gated computed tomography images from 8 patients. We calculated wall thickness and endocardial curvature across the left atrium at end-diastole (ED) then calculated left atrial endocardial area strain throughout the cardiac cycle, using the ED frame as the reference.

The average Pearson's correlation of end-systolic strain with inverse wall thickness and curvature was -0.076 ± 0.095 and 0.017 ± 0.081 respectively. The correlations between inverse wall thickness, curvature and the first four principal components of strain showed no greater dependence of strain on wall thickness or curvature. The LA was divided into 18 regions and correlation was calculated regionally. Regionally, the range of correlation of strain at ES with thickness and curvature was $(-0.58-0.43)$ and $(-0.49-0.47)$ respectively.

Neither wall thickness nor curvature appear to strongly influence strain. This is consistent with either boundary forces acting on the atria or variations in regional stiffness impacting regional differences in strain.

1. Introduction

Atrial fibrosis is a driver for the onset and maintenance of atrial fibrillation, a common arrhythmia which increases the risk of stroke and heart failure. Left atrial (LA) mechanics provide important biomechanical signals for fibrosis.

The law of Laplace states that wall stress in a hollow

pressure chamber is directly proportional to pressure and the radius of curvature, where the radius is the inverse of curvature, and inversely proportional to wall thickness [1]. This law assumes that the thickness of the chamber walls is small relative to the radius. Therefore, in the thin-walled LA chamber, the law of Laplace may provide a reasonable approximation for LA wall stress. The law of Laplace assumes a simplified model of the LA. If a simple linear stiffness model is also assumed, wall stress is proportional to wall strain. We then expect to see a similar dependency of wall strain on wall thickness and curvature, as expressed in the law of Laplace.

The walls of the LA are thin but its thickness and curvature are heterogenous. This may lead to spatial variation in local mechanical behaviours and so, there is uncertainty in the accuracy of the application of the law of Laplace in the atrium. Factors such as LA stiffness, its complex geometry, boundary conditions, as well as active contraction, may also impact the mechanical properties displayed in the LA. Here, we investigate the extent to which curvature and wall thickness may impact LA wall strain using patient-specific models of the LA derived from retrospective gated computed tomography (CT) images.

2. Methods

2.1. Segmentation and Mesh Generation

For each patient, we obtain a representation of LA geometry, segmented from the end-diastolic (ED) CT frame. The high resolution of the CT images allows the heterogenous thickness of the atrial wall to be derived. Images were segmented semi-automatically using a Python script within the freely available Seg3D2 software package [2] as described in [3]. This segmentation script identifies the epicardial and endocardial surfaces using

Hounsfield unit (HU) intensity to discriminate between tissue types.

For segmentation, CT images were cropped to include just the left atrium. A four-point median filter was applied to the images and regions of interest in the LA blood pool and left ventricular (LV) myocardium were selected to determine the HU range for the blood pool and myocardium. An automated script then identified the LA blood pool and the myocardial tissue. A sphere was used for cropping the LA at the mitral valve and separated left atrial myocardium and blood pool from any other labelled structures. The pulmonary veins and LA appendage were cropped from the segmentation so that the segmentation covered the LA body only, allowing for optimum feature tracking [4]. The mitral valve, cropped pulmonary veins and appendage were then labelled.

The cropped and labelled segmentation was used to generate tetrahedral meshes with the Computational Geometry Algorithm Library (CGAL). The atrial anatomies were discretized using tetrahedral elements with mean edge of approximately 260 μm . The endocardial and epicardial surfaces were then identified and extracted from the mesh using Meshtool [5], an open-source code for mesh processing.

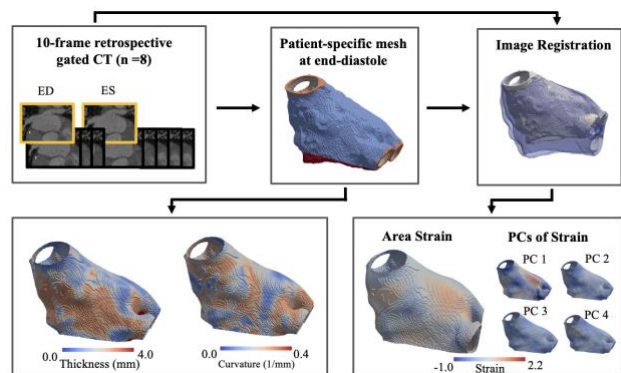


Figure 1. Methods Framework. Patient-specific LA mesh at ED derived from CT. Wall thickness and curvature calculated at reference. Image registration used to estimate LA motion and deform mesh over cardiac cycle. Local area strain used as measure of LA deformation.

2.2 Wall Thickness Calculation

It is challenging to estimate the very small and heterogenous thickness of the LA wall. Here, the method employed is based on the eikonal equation and is implemented using the cardiac arrhythmia research package (CARP) [6,7]. All the vertices on the epicardial surface were activated simultaneously, with the wavefront having a constant, isotropic conduction velocity of 1 mm/s. The thickness of the LA wall was then estimated as the wavefront arrival time at the endocardium. The thickness result was then verified against results from the previously validated but more computationally expensive

Laplace-based method described in [3].

2.3 Curvature Calculation

Meshtool [5] was used to calculate curvature across the LA endocardial surface. The algorithm within Meshtool implements a widely accepted approach using spheres to calculate curvature [8]. To estimate curvature, a circular endocardial surface patch of 5 mm was defined. The method minimizes the distance between the points of the surface patch and the radius of a fitted sphere in a least square sense and curvature is taken as the inverse of the sphere radius. The endocardial surface patch radius was then altered by $\pm 25\%$ to ensure the curvature calculated was independent of patch size and that patch size did not affect the correlations seen.

2.4 Motion Tracking and Strain Calculation

Feature tracking using temporal sparse free-form deformation (TSFFD) registration method with retrospective gated CT [9] has been used to perform feature tracking in the LV. More recently, this method has also been optimized for use in the left atrium [4]. Using this optimized method, reference meshes at end-diastole were deformed to simulate LA motion over the cardiac cycle.

To estimate local deformation in the LV, Pourmorteza et al. calculated the local area strains on the LV endocardial surface from ED to end-systole (ES) [10,11]. Here, instead of LA wall stress, we use strain as a measure of LA deformation from ED to ES as strain can be more readily obtained through calculation from patient CT images. LA area strain in the deformed meshes was estimated as the change in area of the triangular element faces on the endocardial surface as compared to the reference configuration. The area strain at ES was the primary strain metric used here as the maximal degree of deformation from ED is expected at ES.

In addition to area strain at ES, we considered the principal components of strain. The principal components of the local strain transient reduce dimensionality while retaining the maximum amount of information. Hence, we reduced the area strain of each element over the cardiac cycle to the first four principal components which captured $95 \pm 2.1\%$ of the variability of strain over the cardiac cycle.

2.5 Region Definition in Left Atrium

The LA was divided into regions by first defining a coordinate system on the LA. This coordinate system included a rotational coordinate ranging from $-\pi$ at the free wall to 0 in the middle of the septum to π back at the

free wall and a longitudinal coordinate ranging from 0 at the apex to 1 at the base [12]. Using this atrial coordinate system, the LA was divided into 18 regions.

3. Results

3.1. Patient Data and Reference Anatomy

This study was performed using CT images from 8 patients with heart failure indicated for cardiac resynchronization therapy.

For each heart, wall thickness and curvature were calculated from the patient-specific mesh at ED. For each calculation, we obtained maps of wall thickness and curvature patterns across the LA, as shown in Figure 1. The average wall thickness and curvature across 8 models was 1.8 ± 0.42 mm and 0.18 ± 0.078 mm⁻¹ respectively. The pattern of area strain at ES over the LA is also illustrated in Figure 1.

3.2. Global Correlation of Strain with Anatomy

To test if local area strain was related to local wall thickness or curvature, we used Pearson’s correlation coefficient, which provides a measure of the linear relationship between variables.

At ES, we find correlations of (-0.19 to 0.085) between strain and the inverse of wall thickness and correlations of (-0.095 to 0.18) between strain and inverse curvature. The relationship observed between inverse curvature and ES strain was also robust to changing the patch size used in the curvature calculation.

In the law of Laplace, wall stress is proportional to the ratio of the radius of curvature and wall thickness. Therefore, ES strain may show greater dependency on the inverse product of curvature and wall thickness. However, for this case, we saw similar correlations of $r = -0.12$ to 0.10 .

After decomposing the local strain transient into its principal components, the correlations of the principal components of strain with the inverse of wall thickness and curvature were similar to those seen when the ES strain was used. Pearson’s correlation coefficients for all the strain cases are shown in Table 1.

3.3. Correlation of Strain with Anatomy by Region

Given the complex anatomy of the LA and its heterogeneous wall thickness and curvature, the impact of these anatomical features on strain may also vary over the LA. Therefore, considering only a global measure of correlation may not be adequate.

Table 1. Average Pearson’s correlation coefficient of end-systolic strain and principal components of strain (PC) with the inverse of wall thickness (r_{WT}) and curvature (r_C) for $n = 8$ hearts.

Strain	r_{WT}	r_C
End-systolic	-0.076	0.017
PC 1	-0.16	0.018
PC 2	-0.043	0.029
PC 3	-0.020	-0.045
PC 4	-0.034	0.016

Dividing the LA into regions, we looked at the correlation of local area strain at ES with the inverse of wall thickness and curvature within each region. This regional analysis revealed that correlation varies over the LA surface with the range of correlation of strain at ES with the inverse of wall thickness and curvature being (-0.58 to 0.43) and (-0.49 to 0.47) respectively over the 8 hearts. On average, across the 8 hearts, the strongest correlation seen between ES strain and wall thickness was -0.26 (range: -0.58 to -0.024) in the septal region and the strongest correlation between ES strain and curvature was 0.20 (range: -0.18 to 0.43) in the anterior region. There was variability in correlation values among the patient cohort illustrating that there was not a consistent link between regional strain and wall thickness or curvature.

4 Discussion

In this study, the impact of local LA anatomy on local LA wall strain was investigated using CT image-derived motion of the LA over a cardiac cycle. Here, we did not find a correlation between local LA area strain and wall thickness or curvature.

Augustin et al [13] found that principal wall stress in the LA was dependent on wall thickness and curvature during inflation and contraction. In this study, the mechanical behaviour of the LA was simulated in CARP [6,7], while here, LA mechanics were derived from CT images. Limitations arise when simulating LA behaviour from the choice of the electrophysiology model, the model for active contraction, the material model and material parameters as well as from the choice of boundary conditions. Thus, this may explain some of the discrepancy in correlations found. The maximum Spearman’s correlation values between wall stress and inverse thickness and curvature seen in that study were 0.61 and 0.34 respectively. Evaluating the Spearman’s coefficient for wall strain and inverse wall thickness and curvature on our patient cohort did not show an increased dependency of wall strain on wall thickness, $\rho = -0.081 \pm 0.092$, or curvature, $\rho = 0.014 \pm 0.056$, at ES. In [13], only 3 patient cases were considered and despite, the

correlations indicating some dependency of strain on wall thickness and curvature, these correlation values do not suggest that either feature is a dominant factor influencing wall stress.

The law of Laplace has been used to provide a simple approximation for wall stress in the LV, however, there are limitations to this approach [14]. Factors such as the heterogeneous atrial anatomy and the complex arrangement of surrounding structures affecting atrial motion, may further limit suitability of the law of Laplace in the atria.

5. Limitations and Future Work

A major component of this study involves using image registration and retrospective gated CT to deform a reference mesh. TSFFD is a widely used registration method, however, it is possible that alternative registration methods might enhance the accuracy of the atrial motion measurements.

There are also limitations associated with the use of area strain as the measure of atrial deformation. Other metrics such as fiber strain may offer a more physiologically accurate measurement of the strain on the LA wall.

In this investigation, we used data from only 8 patients with heart failure undergoing cardiac resynchronization therapy. We found large ranges in the correlation values reported. As such, it would be valuable to extend this investigation to include a larger cohort with greater diversity, particularly including healthy patients.

6. Conclusion

In this paper, we investigated the influence of wall thickness and curvature on wall strain in patient-specific models of the left atrium on a global and regional scale. There was substantial variability in the Pearson's correlation coefficient calculated across regions and among the cohort of hearts. Despite this variability, the strongest correlations of strain with inverse wall thickness and curvature do not suggest a high dependency of strain on wall thickness or curvature. Factors such as stiffness, the active contraction of the atrium and the boundary conditions imposed by surrounding anatomical structures may play a greater role in determining strain.

Acknowledgements

TMGB is supported by the Leverhulme Doctoral Scholarship Programme – Understanding the mechanics of life.

References

1. Valentinuzzi ME, Kohen AJ. Laplace's law: What it is about, where it comes from, and how it is often applied in physiology [retrospectroscope]. *IEEE Pulse*. 2011 Sep;2(4).
2. Institute SCA. "Seg3D" volumetric image segmentation and visualization. Scientific Computing and Imaging Institute (SCI).
3. Bishop M, Rajani R, Plank G, Gaddum N, Carr-White G, Wright M, et al. Three-dimensional atrial wall thickness maps to inform catheter ablation procedures for atrial fibrillation. *Europace*. 2016;18(3).
4. Sillett C, Razeghi O, Strocchi M, Roney CH, O'Brien H, Ennis DB, et al. Optimisation of Left Atrial Feature Tracking Using Retrospective Gated Computed Tomography Images. In: *Lecture Notes in Computer Science (including subseries Lecture Notes in Artificial Intelligence and Lecture Notes in Bioinformatics)*. Springer Science and Business Media Deutschland GmbH; 2021. p. 71–83.
5. Neic A, Gsell MAF, Karabelas E, Prassl AJ, Plank G. Automating image-based mesh generation and manipulation tasks in cardiac modeling workflows using Meshtool. *SoftwareX*. 2020;11.
6. Vigmond EJ, Hughes M, Plank G, Leon LJ. Computational Tools for Modeling Electrical Activity in Cardiac Tissue. In: *Journal of Electrocardiology*. 2003.
7. Vigmond EJ, Weber dos Santos R, Prassl AJ, Deo M, Plank G. Solvers for the cardiac bidomain equations. Vol. 96, *Progress in Biophysics and Molecular Biology*. 2008.
8. Ji C, Yu J, Li T, Tian L, Huang Y, Wang Y, et al. Dynamic curvature topography for evaluating the anterior corneal surface change with Corvis ST. *Biomed Eng Online*. 2015;14(1).
9. Shi W, Jantsch M, Aljabar P, Pizarro L, Bai W, Wang H, et al. Temporal sparse free-form deformations. *Med Image Anal*. 2013;17(7).
10. Pourmorteza A, Schuleri KH, Herzka DA, Lardo AC, McVeigh ER. A New Method for Cardiac Computed Tomography Regional Function Assessment. *Circ Cardiovasc Imaging*. 2012;5(2).
11. Pourmorteza A, Chen MY, van der Pals J, Arai AE, McVeigh ER. Correlation of CT-based regional cardiac function (SQUEEZ) with myocardial strain calculated from tagged MRI: an experimental study. *International Journal of Cardiovascular Imaging*. 2016;32(5).
12. Bayer J, Prassl AJ, Pashaie A, Gomez JF, Frontera A, Neic A, et al. Universal ventricular coordinates: A generic framework for describing position within the heart and transferring data. *Med Image Anal*. 2018;45.
13. Augustin CM, Fastl TE, Neic A, Bellini C, Whitaker J, Rajani R, et al. The impact of wall thickness and curvature on wall stress in patient-specific electromechanical models of the left atrium. *Biomech Model Mechanobiol*. 2020;19(3).
14. Moriarty T. The law of Laplace. Its limitations as a relation for diastolic pressure, volume, or wall stress of the left ventricle. *Circ Res*. 1980;46(3).

Address for correspondence:

Tiffany MG Baptiste

Department of Biomedical Engineering, King's College London, London, UK

tiffany.baptiste@kcl.ac.uk